

The effect of ^3He impurities on the nonclassical response to oscillation of solid ^4He

E. Kim,^{1,*} J. S. Xia,^{2,3} J. T. West,^{1,†} X. Lin,¹ A. C. Clark,¹ and M. H. W. Chan¹

¹*Department of Physics, The Pennsylvania State University, University Park, Pennsylvania 16802 USA*

²*Department of Physics, University of Florida, Gainesville, Florida 32611 USA*

³*National High Magnetic Field Laboratory (NHMFL), Tallahassee, Florida 32310 USA*

(Dated: April 21, 2022)

We have investigated the influence of impurities on the possible supersolid transition by systematically enriching isotopically-pure ^4He (< 1 ppb of ^3He) with ^3He . The onset of nonclassical rotational inertia is broadened and shifts monotonically to higher temperature with increasing ^3He concentration, suggesting that the phenomenon is correlated to the condensation of ^3He atoms onto the dislocation network in solid ^4He .

PACS numbers: 67.80.-s, 61.72.Ji, 61.72.Lk, 61.72.Hh

The observation of nonclassical rotational inertia (NCRI) in solid helium was first reported in a torsional oscillator (TO) experiment with the solid confined within porous Vycor glass [1]. The NCRI signal is measured as a drop in the resonant period τ_0 of the TO. An intriguing and perhaps counterintuitive result of this experiment is the extreme sensitivity to ^3He impurities in the solid. When a minute concentration of ^3He ($x_3 \approx 10$ ppm) was present the NCRI fraction (NCRIF) showed a 20% decrease. NCRIF is defined by normalizing the apparent mass decoupling in the low temperature limit by the total mass loading of the solid helium sample. The onset temperature T_O (the point where NCRI becomes resolvable from the noise) was found to increase from ~ 175 mK to ~ 300 mK. Increasing x_3 beyond the 10 ppm level continued to increase T_O and decrease NCRIF until, at just $x_3 = 0.1\%$, the signal became undetectable.

NCRI has also been reported in TO measurements on bulk solid ^4He [2, 3, 4, 5, 6, 7, 8, 9]. All studies except one [9] were carried out with commercially available, ultra-high purity (UHP) ^4He solid samples grown using the blocked capillary (BC) method. In all of the data published to date, the temperature dependence in UHP ^4He (both in the bulk [2, 3, 4, 5, 6, 7, 8, 9] and in porous media [1, 10]) is qualitatively reproducible. With decreasing temperature, NCRI gradually emerges from the background near T_O and then rapidly increases before reaching a constant value below a point of saturation T_S . These characteristic temperatures typically fluctuate by a factor of two. In contrast, NCRIF varies widely [5], from 0.03% to at least 20%. It has been suggested that this reflects the degree of disorder in the solid, with higher quality crystals having a smaller NCRIF. However, experimental evidence does not consistently support this notion. For example, although superior growth techniques tend to reduce the effect in a particular TO, NCRIF can still vary by a factor of ten in large crystals grown at constant pressure in two different cells [9].

A different method to study the effects of disorder is to introduce point defects into the crystal. In view of the sensitivity of the phenomenon to ^3He at the parts per

million level [1], we have carried out a systematic study in the bulk phase in which the ^3He concentration was varied from below 1 ppb up to 30 ppm. Two different torsional oscillators were fabricated for this experiment. Measurements of ^4He samples with $1 \text{ ppb} \leq x_3 \leq 129$ ppb were carried out at the high B/T facility of NHMFL at the University of Florida employing a TO (TOF) with $\tau_0 = 0.771$ ms and mechanical quality factor $Q = 1 \times 10^6$. The cylindrical sample space in TOF has a height, $h = 0.50$ cm, and a diameter, $d = 1.00$ cm. The period increases by $\Delta\tau_0 = 3940$ ns upon filling the cell with solid helium at 60 bar. Concentrations in the range, $70 \text{ ppb} \leq x_3 \leq 30$ ppm, were studied at Penn State with another TO (TOP) having $\tau_0 = 1.277$ ms, $Q = 5 \times 10^5$, $h = 0.64$ cm, $d = 0.76$ cm, and $\Delta\tau_0 = 1170$ ns.

The isotopically-pure gas came from the U.S. Bureau of Mines. Similarly purified gas was analyzed [11] and found to have $x_3 < 1$ ppb. There is some uncertainty in the exact concentration of the UHP ^4He . The precise value varies by the source [12] but is always less than 1 ppm. For calculating mixture concentrations we use $x_3 = 300$ ppb for the commercial UHP gas and $x_3 = 1$ ppb for the isotopically-pure gas. Samples with $x_3 < 300$ ppb were prepared by mixing appropriate amounts of the 1 ppb and 300 ppb gases. Samples with $x_3 > 300$ ppb were prepared by mixing 300 ppb gas with pure ^3He . To avoid contamination from residual ^4He a new capillary and room temperature gas handling system were constructed for the isotopically-pure samples. Measurements in each cell started with samples of the lowest x_3 , followed by studies of progressively higher concentrations. The pressure of the solid is determined using an *in situ* resistive strain gauge (resolution ≈ 0.5 bar) attached directly to the outer wall of the torsion cell. The BC method was used for all samples resulting in pressures of 60 ± 5 bar. All of the data were taken during warming scans with low oscillation amplitudes, where the maximum linear speed v_{RLM} of the TO was near or below $10 \mu\text{m s}^{-1}$.

Fig. 1(a) shows NCRIF as a function of temperature for a solid sample with $x_3 = 1$ ppb. NCRI appears below $T_O \approx 80$ mK and saturates below $T_S = 28$ mK. A small

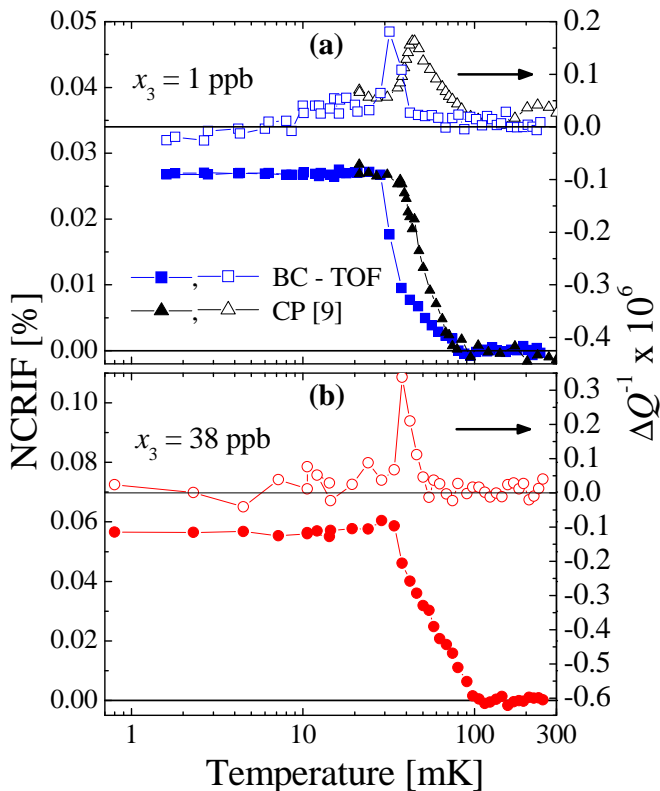


FIG. 1: (a) Comparison of 1 ppb samples from TOF and Ref. [9]. No additional temperature dependence is found below T_S . NCRIF and Q^{-1} data for the CP sample [9] are divided by 12 and 5, respectively. (b) Ultralow temperature scan of a 38 ppb sample from TOF.

dissipation peak is observed with a peak temperature, $T_P = 32$ mK. For $T > T_S$, NCRIF initially drops rapidly and then exhibits a much slower decay to zero between 40 mK and 80 mK. Measurements down to 1 mK reveal no additional features below T_S . Similar behavior is seen at $x_3 = 38$ ppb [see Fig. 1(b)]. Data from a sample ($x_3 = 1$ ppb) grown at constant pressure (CP) in a different cell [9] are also shown in Fig. 1(a). Although the onset temperatures of the two samples are nearly identical, the CP sample (expected to be of much higher quality than the BC sample) shows a sharper transition near T_O .

In Fig. 2 we examine the x_3 dependence of NCRIF measured in the low temperature limit for both this study and for other data obtained at Penn State. Despite the significant shift in the magnitude of NCRIF from cell to cell, the consistent trend is that NCRIF first increases with the impurity concentration and then decreases with further ^3He enrichment beyond ~ 1 ppm.

We compare several solid samples with different x_3 in Fig. 3. NCRIF is normalized to focus on the temperature dependence. Figure 3(a) shows data from TOF. The data presented in Figs. 3(b) and 3(c) are from TOP, with the exception of that obtained [13] with the same annular cell used in Refs. [2, 3]. Both the NCRIF and Q^{-1}

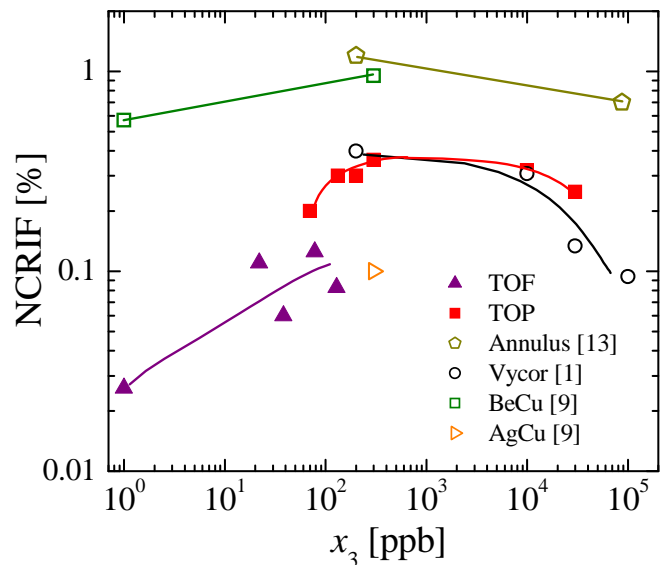


FIG. 2: ^3He dependence of NCRIF for BC samples obtained in this study and in other TO's from our laboratory. There appears to be an optimal concentration of ~ 1 ppm.

(not shown) curves become increasingly broad and shift to higher temperature with increasing ^3He concentration. For samples of overlapping x_3 , data from TOF and TOP are consistent.

Due to the asymptotic decay to zero of NCRIF at high temperature and the rounding near the low temperature saturation point, it is difficult to precisely determine T_O and T_S . To quantitatively compare the temperature dependence in Fig. 3 we have plotted the temperatures, T_x [see Figs. 3(d), 3(e), and 3(f)], at which the normalized NCRIF is $x\%$ (where $x = 10, 50$, or 90) of its low temperature limiting value. The locations of the dissipation peak T_P are also shown, revealing that at low ^3He concentrations $T_P \approx T_{50}$. As x_3 increases so does the value of T_P , but less dramatically than T_{50} . The broadening of the dissipation peak with increasing x_3 is such that no well-defined peak is observable at the highest concentrations. We have compiled the values of T_{50} from this and other experiments into Fig. 4.

One nonsuperfluid mechanism that we have considered as an explanation of the TO experiments is phase separation of the dilute ^3He - ^4He mixtures. We show in Fig. 4 the phase separation boundary according to both experiments [14, 15] and theory [17]. The discrepancy at high x_3 (even for T_{90}) makes it clear that our observations are not the result of phase separation. Although the theoretical boundary at low x_3 crosses the datapoints from this study, there is no experimental evidence [15, 16] of phase separation for $x_3 < 27$ ppm.

It has been proposed [18] that the dependencies of NCRIF on temperature, velocity, and ^3He are the result of a vortex liquid phase, with the true supersolid transition

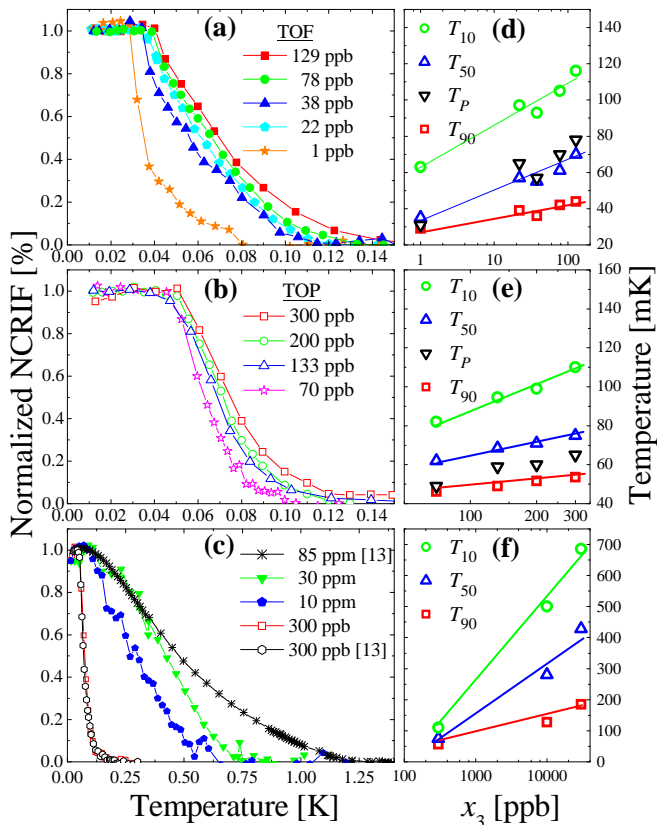


FIG. 3: Temperature dependence of NCRIF (normalized by the low temperature limiting value) for different x_3 grown in (a) TOF and (b) TOP. (c) Temperature dependence for $x_3 \geq 300$ ppb. Two traces obtained with an annular cell [13] are also shown. (d), (e), (f) The right three panels show the x_3 dependencies of the characteristic temperatures, which were extracted from the adjacent plots.

occurring at lower temperature. In this context, the high temperature tail reflects the finite response time of vortices in the sample to oscillatory motion. The broadening with increasing x_3 (see Fig. 3) is due to the slowed vortex motion when ^3He atoms attach to the normal cores and get dragged along with the vortices. The accompanying dissipation peak signifies the matching of the TO resonant frequency and the optimal rate at which vortices can respond to changes in the velocity field. Thus, the x_3 dependence of T_P (which is similar to that of T_x) may be a direct probe of the drag force caused by ^3He impurity atoms. The complete saturation of NCRIF below T_S (see Fig. 1) indicates that, if there is a supersolid phase of ^4He , the critical temperature T_C is either less than 1 mK or is such that $T_S < T_C < T_O$.

The similarities between vortices and dislocations have been discussed recently [19]. Thus, another process that we consider is the condensation (evaporation) of ^3He atoms onto (from) dislocation lines within the sample upon cooling (warming) [20, 21]. Dislocations in solid ^4He form a random three-dimensional network in which

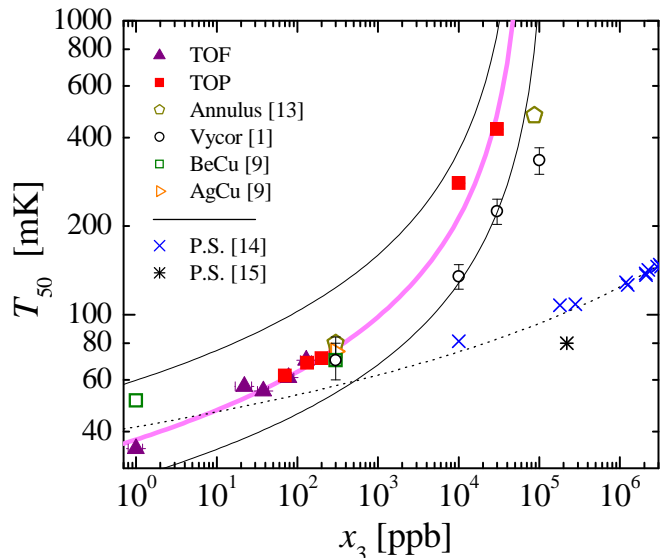


FIG. 4: T_{50} versus x_3 . Relative to T_{50} , values of T_{10} and T_{90} (excluded for clarity) are shifted vertically upward by $\sim 60\%$ and downward by $\sim 25\%$, respectively. From top to bottom, the three solid lines represent the condition, $T_{IP} = T_x$, for $x = 10, 50$, and 90 . To apply Eq. (1) we assume that all samples have the same L_N (and Λ). The fitting parameters are listed in Table I. The theoretical phase separation boundary [17] (dotted line), anchored by pressure [14] and ultrasound [15] measurements, is inconsistent with the TO data.

the lines intersect with one another to form a vast number of nodes, which are essentially immobile. In contrast, the line segments between nodes can move readily in stress fields. When an oscillating stress field is imposed, the dislocation segments vibrate with little or no damping below 1 K [22]. The network is characterized by the total line density Λ (total dislocation line length per unit volume) and network loop length L_N between nodes. From ultrasound measurements of single crystals [20, 22, 23], it is usually found that $0.1 < \Lambda L_N^2 < 0.2$, where $\Lambda \approx 1 \times 10^6 \text{ cm}^{-2}$ and $L_N \approx 5 \mu\text{m}$. In crystals grown with the BC method it is expected that Λ will increase and L_N will decrease. At low temperature ^3He atoms bind to the dislocations with an energy E_B and act as additional pinning centers. There is a crossover from network-pinning to impurity-pinning when the average distance L_{IP} between condensed ^3He atoms becomes less than L_N . The

TABLE I: Parameters for Eq. (1) that are associated with the three curves in Fig. 4. Uncertainties in E_B are 10%, and in L_N they are 20%. The dislocation densities were calculated by setting $L_N \approx L_{IP}$ and $\Lambda L_N^2 = 0.2$.

T_x [K]	E_B [K]	L_{IP} [μm]	Λ [10^7 cm^{-2}]
T_{10}	0.66	1.7	0.7
T_{50}	0.42	1.8	0.6
T_{90}	0.33	1.3	1.2

x_3 -dependent temperature at which this occurs can be obtained from the average pinning length [20], and is of the form

$$T_{IP} = -2E_B \left(\ln \left[\frac{x_3^2 L_{IP}^3 E_B}{4\mu b^6} \right] \right)^{-1}. \quad (1)$$

Here, b is the magnitude of the Burger's vector of a dislocation and μ is the shear modulus of ^4He .

In order to reveal the possible connection between ^3He impurity-pinning and the observed x_3 dependence of NCRI, we identify the crossover point with each of the characteristic temperatures (i.e., $T_{IP} = T_x$) and fit the measured T_{10} , T_{50} , and T_{90} by adjusting the parameters L_{IP} and E_B . Figure 4 demonstrates the accuracy of Eq. (1) in describing T_{50} versus x_3 . The best fit parameters, which are consistent with those found in the literature [20, 21], are listed in Table I. If we fix $E_B = 0.42$ K for all three datasets, the curves calculated from Eq. (1) deviate from the observed T_{10} and T_{90} for $x_3 < 100$ ppb. However, such a protocol results in L_{IP} that are longest for T_{10} and shortest for T_{90} , as expected [20]. The same qualitative trends are observed in the Vycor data. However, the above analysis is inappropriate due to the solid ^4He morphology [24] and overall complexity of the system. If we naively apply Eq. (1) we get parameters similar to those in Table I (eg., for T_{50} we get $L_{IP} = 0.5 \mu\text{m}$, which is much greater than the 7 nm pore size).

The fact that the characteristic temperatures of NCRI can be described by Eq. (1) indicates that the observed x_3 dependence is correlated with the impurity-pinning of dislocations. The temperature independence for $1 \text{ mK} < T < T_S$ (see Fig. 1) suggests that below the saturation point the dislocations are completely pinned. It is surprising that even just 1 ppb (or less [11]) of impurities can immobilize the dislocations. As a sample of a fixed x_3 is warmed above T_S the continual evaporation of ^3He atoms from the dislocation network softens the solid, which may concomitantly destroy NCRI. A dramatic increase at low temperature of the shear modulus in solid ^4He has in fact been observed recently [25]. The anomaly exhibits the same qualitative (and perhaps quantitative) dependencies on temperature, ^3He concentration (for $x_3 = 1$ ppb, 85 ppb, and 300 ppb), and stress amplitude ($\propto v_{RIM}$ in the TO experiments) as NCRI. We are further investigating the connection between these experiments.

In conclusion, we found that the x_3 dependence of the characteristic temperatures of NCRI are consistent with the binding of ^3He atoms to dislocations. The absence of any temperature dependence below ~ 28 mK in isotopically-pure samples suggests that the most likely phase transition point lays between T_S and T_O .

We thank P. W. Anderson and J. R. Beamish for their advice. E. K. and M. H. W. C. also acknowledge the illuminating discussions at workshops held at the Kavli Institute of Theoretical Physics at UCSB (2006), the As-

pen Center for Physics (2006), Keio University (2007), and the Outing Lodge sponsored by the Pacific Institute of Theoretical Physics (2007). The work at PSU was supported by USA NSF grants DMR-0207071 and DMR-0706339. The State of Florida and USA NSF DMR-9527035 funded research carried out at UF.

* Permanent address: Physics Department, Korea Advanced Institute of Science and Technology (KAIST), 373-1 Guseong-dong, Yuseong-gu, Daejeon 305-701, Korea

† Electronic address: jtw11@psu.edu

- [1] E. Kim and M. H. W. Chan, *Nature* **427**, 225 (2004).
- [2] E. Kim and M. H. W. Chan, *Science* **305**, 1941 (2004).
- [3] E. Kim and M. H. W. Chan, *Phys. Rev. Lett.* **97**, 115302 (2006).
- [4] A. S. C. Rittner and J. D. Reppy, *Phys. Rev. Lett.* **97**, 165301 (2006).
- [5] A. S. C. Rittner and J. D. Reppy, *Phys. Rev. Lett.* **98**, 175302 (2007).
- [6] Y. Aoki, J. C. Graves, and H. Kojima, *Phys. Rev. Lett.* **99**, 015301 (2007).
- [7] A. Penzev, Y. Yasuta, and M. Kubota, *J. Low Temp. Phys.* **148**, 677 (2007).
- [8] M. Kondo, S. Takada, Y. Shimbayama, K. Shirahama, **148**, 695 (2007).
- [9] A. C. Clark, J. T. West, and M. H. W. Chan, *Phys. Rev. Lett.* **99**, 135302 (2007).
- [10] E. Kim and M. H. W. Chan, *J. Low Temp. Phys.* **138**, 859 (2005).
- [11] See reports BM-RI-8054, BM-RI-9010, and PB-86-205309/XAB.
- [12] Additional numbers and references can be found at <http://www.grisda.org/origins/25055.htm>.
- [13] E. Kim, Ph.D. Thesis, The Pennsylvania State University, 2004.
- [14] A. N. Gan'shin *et al.*, *Low Temp. Phys.* **26**, 869 (2000).
- [15] J. M. Goodkind, *AIP Conf. Proc.* **850**, 329 (2006).
- [16] X. Lin, A. C. Clark, and M. H. W. Chan, accepted for publication in *Nature* (London) (2007).
- [17] D. O. Edwards and S. Balibar, *Phys. Rev. B* **39**, 4083 (1989).
- [18] P. W. Anderson, *Nature Phys.* **3**, 160 (2007).
- [19] M. Boninsegni, A. B. Kuklov, L. Pollet, N. V. Prokof'ev, B. V. Svistunov, and M. Troyer, *Phys. Rev. Lett.* **99**, 035301 (2007); A.C. Clark and M. H. W. Chan, to be published (2007).
- [20] I. Iwasa and H. Suzuki, *J. Phys. Soc. Jpn.* **49**, 1722 (1980).
- [21] M. A. Paalanen, D. J. Bishop, and H. W. Dail, *Phys. Rev. Lett.* **46**, 664 (1981).
- [22] R. Wanner, I. Iwasa, and S. Wales, *Solid State Commun.* **18**, 853 (1976).
- [23] I. Iwasa, K. Araki, and H. Suzuki, *J. Phys. Soc. Jpn.* **46**, 1119 (1979).
- [24] D. Wallacher, M. Rheinstaedter, T. Hansen, and K. Knorr, *J. Low Temp. Phys.* **138**, 1013 (2005).
- [25] J. Day and J. R. Beamish, accepted for publication in *Nature* (London) (2007); arXiv:0709.4666v1 (2007).